

# REMOVAL OF ORGANIC DYES FROM CONTAMINATED WATER USING $\text{CoFe}_2\text{O}_4$ /REDUCED GRAPHENE OXIDE NANOCOMPOSITE

F. Sakhaei<sup>\*1</sup>, E. Salahi<sup>1</sup>, M. Eolya<sup>2</sup> and I. Mobasherpour<sup>1</sup>

<sup>\*</sup>f.sakhaii@gmail.com

Received: April 2016

Accepted: November 2016

<sup>1</sup> Ceramic Department, Materials and Energy Research Center, Karaj, Iran.

<sup>2</sup> Department of Environmental Research, Institute for Color Science and Technology, Tehran, Iran.

**Abstract:** Up to now, lots of materials such as active carbon, iron, manganese, zirconium, and metal oxides have been widely used for removal of dyes from contaminated water. Among these, ferrite nanoparticle is an interesting magnetic material due to its moderate saturation magnetization, excellent chemical stability and mechanical hardness. Graphene, a new class of 2D carbonaceous material with atom thick layer features, has attracted much attention recently due to its high specific surface area. Reduced graphene oxide (rGO) has also been of great interest because of its unique properties, which are similar to those of graphene, such as specific surface area, making it an ideal candidate for dye removal. Thus far, few works have been carried out on the preparation of  $\text{CoFe}_2\text{O}_4$ -rGO composite and its applications in removal of contaminants from water. In this paper,  $\text{CoFe}_2\text{O}_4$  reduced graphene oxide nanocomposite was fabricated using hydrothermal process. During the hydrothermal process, the reduction of graphene oxide and growth of  $\text{CoFe}_2\text{O}_4$  simultaneously occurred on the carbon basal planes under the conditions generated in the hydrothermal system. The samples were characterized by X-ray diffraction (XRD), scanning electron microscopy (SEM), and Fourier transform infrared spectroscopy contaminant and UV-Vis spectroscopy as the analytical method. The experimental results suggest that this material has great potential for treating Congo red contaminated water.

**Keywords:** Dye, graphene, nanocomposite, removal.

## 1. INTRODUCTION

$\text{CoFe}_2\text{O}_4$  belongs to the family of spinel ferrite and is one of the most important ferrites for high density magneto optic recording applications due to its high coercivity, moderate magnetization, very high magneto crystalline anisotropy, chemical stability and mechanical hardness [1].  $\text{CoFe}_2\text{O}_4$  has been extensively studied in the removal of toxic ions and organic pollutants from water. This compound shows higher removal capacity than the bulk materials due to its high electromagnetic performance, excellent chemical stability, mechanical hardness and photocatalytic activity [1-4].

As proved by many researchers, graphene and reduced graphene oxide effectively remove dyes because of their two dimensional structure, high specific surface area (theoretically ~2600 m<sup>2</sup>/g), good chemical stability and other excellent properties [5-8].

The synthetic dyes are used for industrial dyeing such as textile, leather, and cosmetics. It is estimated that 10-15% of these dyes are lost in

the effluents during dyeing process. The discharge of dye wastewater into natural streams and rivers cause severe problems because it is toxic to the aquatic life and causes damages to the environment [9-12].

Therefore, it is necessary to remove these contaminants from water. For this purpose, in this paper,  $\text{CoFe}_2\text{O}_4$ /reduced graphene oxide nanocomposite was prepared by hydrothermal method and then the removal of Congo red from contaminated water using this compound was investigated.

## 2. EXPERIMENTAL

In this paper, GO was prepared using modified Hummers method[8]. Dispersed GO was then mixed with  $\text{Co}^{2+}$  and  $\text{Fe}^{3+}$  with a molar ratio of 1:2. After 12 hours, the pH of the resulting suspension was adjusted to 10 using ammonium hydroxide aqueous solution. Subsequently, the obtained precipitate was transferred into a stainless steel autoclave and kept at 180 °C and a pressure of 11 bar for 10 h. The resulting

nanocomposite was washed by deionized water several time and dried under vacuum at 60 ° C. During the hydrothermal process the reduction of graphene oxide and the growth of  $\text{CoFe}_2\text{O}_4$  simultaneously occurred on the carbon basal planes under the conditions generated in the hydrothermal system. The samples were characterized by X-ray diffraction (XRD), scanning electron microscopy (SEM), and Fourier transform infrared spectroscopy (FT-IR).

### 3. RESULTS AND DISCUSSION

#### 3. 1. Characterization

Functionalization and detection of oxidized graphite were studied by infrared spectrum of graphite and graphite oxide, shown in Figure 1. In this spectrum, the peaks at 2922 and 2860  $\text{cm}^{-1}$  belong to the symmetric and asymmetric stretching vibrations of  $\text{CH}_2$ , respectively. The peaks at 3441  $\text{cm}^{-1}$  and the sharp peak at 1626  $\text{cm}^{-1}$  correspond to the stretching vibration of OH- and water absorption by graphene oxide, respectively. The peak in 1620-1626  $\text{cm}^{-1}$  range is attributed to non-oxide C=C group. The peaks at 1741 and 1380, 1226-1228, 1089 and 1055 are related to C=O, C-O epoxy and alkoxy, respectively. In

addition, the peaks in the range of 1225-1226  $\text{cm}^{-1}$  and 1230  $\text{cm}^{-1}$  can be related to carboxylic O-H, too. In conclusion, this spectrum shows that graphite has been oxidized and consists of O-H and oxygen containing functional groups. In the infrared spectrum of reduced graphene oxide by the hydrothermal method, the peaks at 1620  $\text{cm}^{-1}$  and the sharp peak at 3440  $\text{cm}^{-1}$  in FTIR spectra of graphene oxide are associated with the stretching vibration of O-H have substantially reduced, indicating that this functional group has been omitted during the process. In addition, the absence of a peak at 1741  $\text{cm}^{-1}$ , corresponding to the stretching vibration of C=O in FTIR spectrum of reduced graphene oxide shows the reduction of this functional group. The peak at 1224  $\text{cm}^{-1}$  could be related to epoxy and the new peak at 1562  $\text{cm}^{-1}$  is related to stretching vibration of reduced graphene oxide skeleton [5-8, 13].

In Figure 1, some peaks at 1634  $\text{cm}^{-1}$  and 3405/32  $\text{cm}^{-1}$  are related to water absorption on the surface of nanoparticles and the strong peaks in the range of 500-600  $\text{cm}^{-1}$  are related to Fe-O bonds and those in 500-800  $\text{cm}^{-1}$  range are attributed to Co-O bands [2, 3].

X-ray diffraction pattern for synthesized ferrite cobalt (Figure 2-a) shows the formation of cubic spinel type (JCPDS1000-1121) in all cases [2, 3].

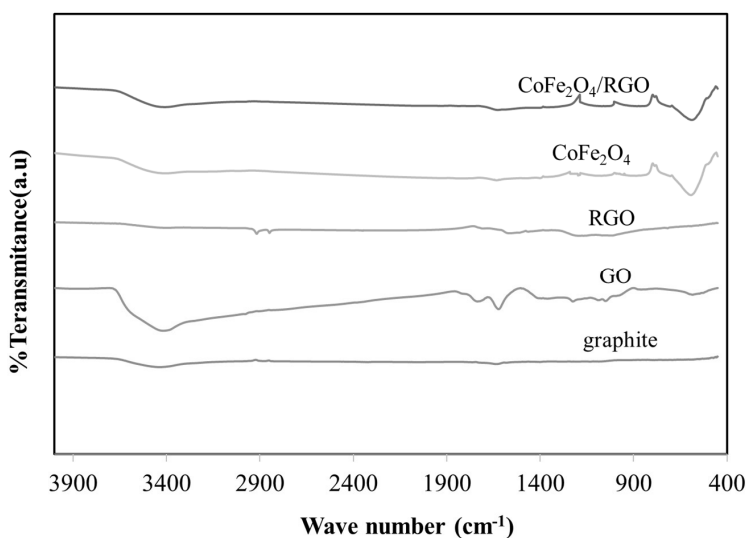


Fig. 1. FTIR spectra of graphite, GO, RGO, pure  $\text{CoFe}_2\text{O}_4$ , RGO and  $\text{CoFe}_2\text{O}_4$  nanocomposite

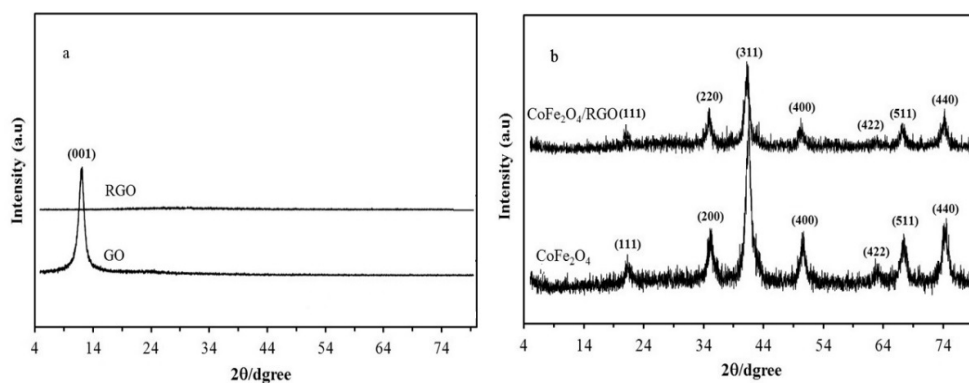


Fig. 2. XRD patterns of the samples

In the X-ray diffraction pattern of ferrite cobalt reduced graphene oxide composite, the ferrite cobalt peaks are quite visible. However, there is no peak related to reduced graphene oxide due to reduction of graphene oxide during hydrothermal process and simultaneous growth of ferrite on graphene sheets. Graphene sheets are quite covered by cobalt ferrite. Therefore, the intermolecular interactions, Vander-Waals force

and  $\pi$ - $\pi$  interactions between graphene sheets are prohibited by ferrite nanoparticles. As a result, reduced graphene oxide sheets show no peak of (0 0 2). Moreover, low weight ratio of graphene oxide can be another reason. This is notably consistent with other researchers' reports. The selection of raw materials for the formation of desired cation complex is appropriate and the complex is expected to dissociate as a result of

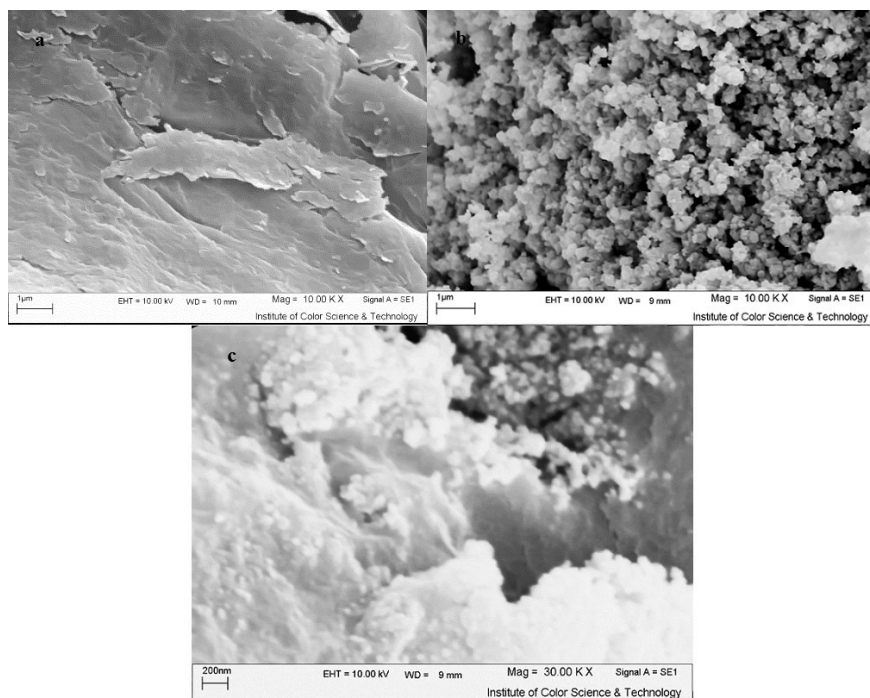


Fig. 3. Typical SEM images of the as synthesized GO, CoFe<sub>2</sub>O<sub>4</sub> RGO and CoFe<sub>2</sub>O<sub>4</sub> nanocomposites

temperature and pressure under hydrothermal conditions to ultimately obtain ferrite cobalt. [2, 3, 13-16].

Figure 3 (a, b and c) shows the SEM images of the graphene oxide, ferrite and ferrite reduced graphene oxide nanocomposite. It can be observed that the nanoparticle and nanosheets have the tendency to agglomerate as a result of the widespread distribution of nanoparticles and the existence of a lot of pores in samples can be related to the presence of the gas at high temperatures.

Observation of the synthesized nanocomposites images (ferrite cobalt reduced graphene oxide) shows that there are plenty of spaces with hydrothermal method and the particles are about 20 nm on the surface and edges (Figure 3c). Comparing the nanocomposite of ferrite and reduced graphene oxide after and before reduction by hydrothermal method, there are some changes in size; especially in graphene

morphology. In addition, it seems that placing nanoparticles between the sheets can decrease their accumulation. Narrower distribution, more uniform and smaller particle size of synthesized ferrite nanoparticles in SEM images suggest that graphene sheets were effective on dispersing nanoparticles[1, 17].

### 3. 2. The Effect of Nanocomposite on the Contaminated Water

Figure 4a shows the ferrite-graphene effect in the absence of UV light, indicating that no considerable absorptions occur on the nanocomposite surface.

The effect of ferrite alone on bleaching in Figure 4b shows that only 40% decolorization has taken place within an hour.

The effect of  $\text{CoFe}_2\text{O}_4$ / reduced graphene oxide nanocomposite on removal of Congo red dye under UV irradiation is shown in Figure 4c.

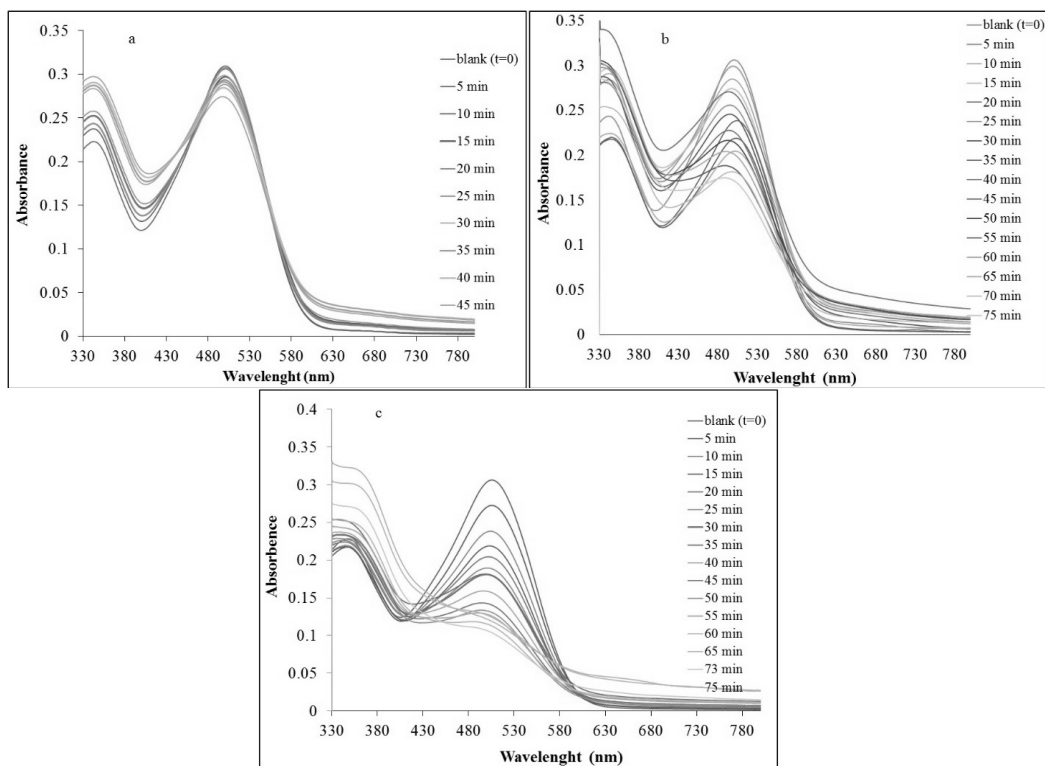


**Fig. 4.** Absorption spectra of Congo red aqueous solution (10 ppm) at temptation of 25°C and natural pH  $\text{CoFe}_2\text{O}_4$ / reduced graphene oxide nanocomposite in dark (a),  $\text{CoFe}_2\text{O}_4$  under UV light (b) and  $\text{CoFe}_2\text{O}_4$ / reduced graphene oxide nanocomposite (c)

UV irradiation on dye solution in the presence of nanocomposites causes in dye concentration and the decrease of absorption band of dye in visible region. In this way, decolorization percentage reached 68% in about one hour. Finally, the band in the ultraviolet region located at about 350 nm is increasing due to the naphthalene ring. Therefore, this may be related to the beginning of degradation of Congo red dye in this time.

In addition, the comparison of diagrams 4a and 4c shows that CoFe<sub>2</sub>O<sub>4</sub> reduced graphene oxide nanocomposite has a higher capability of decolorization than ferrite during the same time period. Moreover, lack of variations in the wavelengths in ferrite UV spectrum (Fig 4b) indicates that the decomposition process has not yet begun in this time period, which may probably be attributed to the electron-hole recombination by narrowing of the gap [18-20].

#### 4. CONCLUSION

In this research, CoFe<sub>2</sub>O<sub>4</sub> /reduced graphene oxide nanocomposite has been successfully prepared via hydrothermal method. SEM images indicate the uniform distribution of nanoparticle on the carbon basal planes under the conditions generated in the hydrothermal system. The XRD pattern of nanocomposite proved the forming spinel type ferrite. Highly efficient removal of Congo red dye under UV irradiation suggests a potential application of this nanocomposite.

#### ACKNOWLEDGMENT

In this work was supported by Ceramic Department, Energy Research Center and Department of Environmental Research, Institute for Color Science and Technology

#### REFERENCES

1. Dong, M., Lin, Q., Chen, D., Fu X., Wang, M., Wu, Q., Chen, X. and Li, S., "Amino acid-assisted synthesis of superparamagnetic CoFe<sub>2</sub>O<sub>4</sub> nanostructures for the selective adsorption of organic dyes". RSC Advances., 2013, 3, 11628-11663.
2. Fu, Y., Chen, H., Sun, X., Wang, X., "Combination of cobalt ferrite and graphene: High-performance and recyclable visible-light photocatalysis". Applied Catalysis B: Environmental., 2012, 111-112, 280-287.
3. Li, S., Wang, B., Liu, J. and Yu, M., "In situ one-step synthesis of CoFe<sub>2</sub>O<sub>4</sub>/graphene nanocomposites as high-performance anode for lithium-ion batteries". Electrochimica Acta., 2014, 129, 33-39.
4. Yao, Y., Yang, Z., Zhang, D., Peng, W., Sun, H. and Wang, S., Magnetic CoFe<sub>2</sub>O<sub>4</sub>-graphene hybrids: facile synthesis, characterization, and catalytic properties. Industrial & Engineering Chemistry Research., 2012, 51, 6044-6051.
5. Pei, S. and Cheng, H-M., "The reduction of graphene oxide". Carbon., 2012, 50, 3210-3228.
6. Dreyer, D. R., Park, S., Bielawski, C. W. and Ruoff, R. S., "The chemistry of graphene oxide". Chemical Society Reviews., 2010, 39, 228-240.
7. Mermoux, M., Chabre, Y. and Rousseau, A., "FTIR and <sup>13</sup>C NMR study of graphite oxide". Carbon., 1991, 29, 469-474.
8. Marcano, D. C., Kosynkin, D. V., Berlin, J. M., Sinitskii, A., Sun, Z., Slesarev, A., Alemany, L. B., Lu, W. and Tour, J. M., "Improved Synthesis of Graphene Oxide". ACS Nano., 2010, 4, 4806-4814.
9. Koprivanac, N. and Kušić H., "Hazardous organic pollutants in colored wastewaters". Nova Science Publishers., Inc.; ENG, 2009.
10. Máximo, C., Amorim, M. T. P. and Costa-Ferreira, M., "Biotransformation of industrial reactive azo dyes", by Geotrichum sp. CCM1 1019. Enzyme and Microbial Technology., 2003, 32, 145-151.
11. Sathishkumar, P., Mangalaraja, R. V., Anandan, S. and Ashokkumar, M., "CoFe<sub>2</sub>O<sub>4</sub>/TiO<sub>2</sub> nanocatalysts for the photocatalytic degradation of Reactive Red 120 in aqueous solutions in the presence and absence of electron acceptors". Chemical Engineering Journal., 2013, 220, 302-310.
12. Marandi, R., Olya, M. E., Vahid, B., Khosravi, M. and Hatami, M., "Kinetic modeling of photocatalytic degradation of an azo dye using nano-TiO<sub>2</sub>/polyester". Environmental Engineering Science., 2012, 29, 957-963.

13. Chandra, V., Park, J., Chun, Y., Lee, J. W., Hwang, I-C. and Kim, K. S., "Water-Dispersible Magnetite-Reduced Graphene Oxide Composites for Arsenic Removal". *ACS Nano.*, 2010, 4, 3979- 3986.
14. Wang, X., Tian, H., Yang, Y., Wang, H., Wang, S., Zheng, W. and Liu, Y., "Reduced graphene oxide/CdS for efficiently photocatalytic degradation of methylene blue". *Journal of Alloys and Compounds.*, 2012, 524, 5-12.
15. Li, W., Qiao, X., Zheng, Q. and Zhang, T., "One-step synthesis of  $MFe_2O_4$  ( $M = Fe, Co$ ) hollow spheres by template-free solvothermal method". *Journal of Alloys and Compounds.*, 2011, 509, 6206-6211.
16. Kumar, P. R., Kollu, P., Santhosh, C., Eswara Varaprasada Rao, K., Kim, D. K. and Grace, A. N., "Enhanced properties of porous  $CoFe_2O_4$ -reduced graphene oxide composites with alginate binders for Li-ion battery applications". *New Journal of Chemistry.*, 2014, 38, 3654-3661.
17. Zhou, L., Deng, H., Wan, J., Shi, J. and Su, T., "A solvothermal method to produce RGO- $Fe_3O_4$  hybrid composite for fast chromium removal from aqueous solution". *Applied Surface Science.*, 2013, 283, 1024-1031.
18. Mahmoodi, N. M., "Photocatalytic ozonation of dyes using copper ferrite nanoparticle prepared by co-precipitation method". *Desalination.*, 2011, 279, 332-337.
19. Lan, M., Fan, G., Sun, W. and Li, F., "Synthesis of hybrid Zn-Al-In mixed metal oxides/carbon nanotubes composite and enhanced visible-light-induced photocatalytic performance". *Applied Surface Science.*, 2013, 282, 937-946.
20. Shu, X., He, J., Chen, D. and Wang, Y., "Tailoring of phase composition and photoresponsive properties of Ti-containing nanocomposites from layered precursor". *The Journal of Physical Chemistry C.*, 2008, 112, 4151-4158.